

Coherent Optical Phonons in the Iron Oxypnictide



Hiroshi TAKAHASHI¹, Yoichi KAMIHARA^{2,3}, Hiroaki KOGUCHI¹, Toshiyuki ATOU¹, Hideo HOSONO^{1,4},
Ikufumi KATAYAMA⁵, Jun TAKEDA⁵, Masahiro KITAJIMA⁶, and Kazutaka G NAKAMURA¹

¹*Materials and Structures Laboratory, Tokyo Institute of Technology, Yokohama 226-8503, Japan*

²*Department of Applied Physics and Physico-Informatics, Faculty of Science and Technology, Keio University, Yokohama 223-8522, Japan*

³*JST, TRIP, Chiyoda, Tokyo 102-0075, Japan*

⁴*Frontier Reserch Center, Tokyo Institute of Technology, Yokohama 226-8503, Japan*

⁵*Faculty of Engineering, Yokohama National University, Yokohama 240-8501, Japan*

⁶*National Defense Academy of Japan, Yokosuka, Kanagawa 239-8686, Japan*

(Received July 27, 2010; accepted November 8, 2010)

Coherent optical phonons with the Fe-related mode $B_{1g}(\text{Fe})$ in the iron oxypnictide $\text{SmFeAsO}_{1-x}\text{F}_x$ ($x = 0.075$) are observed using femtosecond time-resolved reflection measurements with electrooptic sampling, in addition to the $A_{1g}(\text{Sm})$ and $A_{1g}(\text{As})$ modes. The time evolution of the frequency and amplitude of optical phonons is studied and the lifetimes of phonons are estimated. The frequency softening and positive frequency chirp related to the strong carrier–phonon coupling are found for the $A_{1g}(\text{Sm})$ mode.

KEYWORDS: iron oxypnictide, coherent phonons, femtosecond laser

Iron pnictides have recently gained considerable attention since superconductivity was observed for F-doped samples.¹⁻¹²⁾ Understanding the mechanism of high-temperature superconductivity is one of the most important open issues in condensed matter physics, and the role of carrier–phonon coupling in unconventional superconductivity is still controversial. Various measurement techniques have been used to characterize and analyze the structures and functions of iron pnictides. Spectroscopic measurements using conventional Raman scattering and infrared absorption have also been conducted, and vibrational structures and phonon modes have been revealed.⁹⁻¹²⁾ However, the available Raman data do not show any evidence of strong electron–phonon coupling in terms of phonon lineshape and linewidth,¹¹⁻¹³⁾ although the isotope effect of iron on superconducting and spin-density-wave (SDW) transitions has been observed.^{14,15)} The dynamics of phonons including phonon–phonon and carrier–phonon couplings are usually studied by time domain spectroscopy using femtosecond time-resolved reflection or transmission measurements.^{16,17)} When the femtosecond laser pulse, whose duration is much shorter than the vibrational period of target materials, interacts with the sample, phonons are excited coherently. The coherently excited phonons are called coherent phonons. The transient polarization caused by the coherent phonons can be detected as a change in time-evolved reflection or transmission signal if we measure them in a femtosecond time domain. The measurements of coherent phonons have been conducted for various materials, such as semiconductors, semimetals, and oxides,^{16,17)} and revealed the dynamics of phonon–phonon and carrier–phonon couplings. However, coherent phonons of very few superconductors have been studied.¹⁸⁻²⁴⁾ Very recently, coherent optical phonons have been studied in iron oxypnictides; however, only the A_{1g} mode was reported.^{23,24)} The coherent phonons with the iron-related mode, which is considered to be much more important in exploring the superconducting and SDW mechanism for iron-based compounds,¹²⁾ have yet to be observed.^{23,24)}

In this letter, we first report the observation of coherent phonons in the iron pnictide $\text{SmFeAsO}_{1-x}\text{F}_x$ ($x = 0.075$) using the femtosecond transient reflection measurement. In addition to the $A_{1g}(\text{Sm})$ and $A_{1g}(\text{As})$ modes, the Fe-related phonon mode $B_{1g}(\text{Fe})$ is clearly observed. The frequency chirp in the coherent phonons, which is related to phonon–phonon and carrier–phonon couplings, is also found in the A_{1g} mode.

The sample used was $\text{SmFeAsO}_{1-x}\text{F}_x$ ($x = 0.075$). Polycrystalline samples were prepared by a two-step solid-state reaction in a sealed silica tube using dehydrated Sm_2O_3 and a mixture of compounds composed of SmAs , Fe_2As , and FeAs ($\text{SmAs–Fe}_2\text{As–FeAs}$ powder) as starting materials. The dehydrated Sm_2O_3 was prepared by heating a commercial Sm_2O_3

powder (Rare Metallic, 99.99 wt %) at 1000 °C for 5 h in air. To obtain the SmAs–Fe₂As–FeAs powder, Sm (Nippon Yttrium, Sm with purity 99.9 wt %), Fe (Kojundo Chemical Laboratory, > 99.9 wt %), and As (Kojundo Chemical Laboratory, 99.9999 wt %) were mixed in a stoichiometric ratio of 1:3:3 and heated at 850 °C for 10 h in an evacuated silica tube. Then, a 1:1 mixture of the two powders (dehydrated Sm₂O₃ and SmAs–Fe₂As–FeAs powders) was pressed and heated in a sealed silica tube at 1300 °C for 15 h to obtain a sintered pellet. To prevent the silica tube from collapsing during the reaction, the tube was filled with high-purity Ar gas with a pressure of 0.2 atm at room temperature. All procedures were carried out in an Ar-filled glove box (MIWA Mfg; O₂, H₂O < 1 ppm). F doping was performed by replacing part of Sm₂O₃ with SmF₃ (Rare Metallic, 99.99 wt %) and adding a stoichiometric Sm metal in the starting materials.⁷⁾ The T_c of the sample was 51.08 K.⁷⁾

Pump–probe reflection measurements were performed using the mode-locked Ti:sapphire laser source. The pulse width, the center wavelength, and the repetition rate were 40 fs, 800 nm, and 86 MHz, respectively. The photon energy of 1.55 eV allowed a vertical transition across the optical band gap of SmFeAsO_{1-x}F_x ($x = 0.075$) at room temperature. The intensities of the pump and probe pulses were 77 and 21 μJ/cm², respectively. The photoexcited carrier density was estimated to be 6×10^{19} cm⁻³ using an absorption length of 37 nm, which is obtained for LaAsFeO²⁾ because that for SmAsFeO has not been reported. For detection, the electrooptic (EO) sampling configuration was used. In this sampling configuration, the polarization of the pump is normal (s-polarization), and that of the probe beam is 45° with respect to the optical plane.¹⁷⁾ After the reflection from the sample, the probe beam was classified into s- and ppolarized components, and detected with matched photodiodes. By taking the difference between the two photocurrents $\Delta R(t) = \Delta R_s(t) - \Delta R_p(t)$, we eliminated the isotropic response, in order to record the much weaker anisotropic reflectivity components. The time delay t between pump and probe pulses was modulated at 20 Hz to enable accumulation and averaging of typically 12,000 scans with a digital oscilloscope.

Figure 1 shows a typical transient reflection signal $\Delta R(t)/R$ in a photoexcited SmFeAsO_{1-x}F_x ($x = 0.075$). There is a coherent oscillation due to optical phonons after a strong response at $t=0$. Figure 2 shows the Fourier transform (FT) spectrum of the transient reflection signal. There are three peaks: one strong peak at 5.0 THz and two weak peaks at 6.0 and 6.4 THz. The structure of SmFeAsO belongs to the $P4/nmm$ space group. Formal group analysis gives eight Raman active modes: $2A_{1g} + 2B_{1g} + 4E_g$.^{11,12)} The A_{1g} and B_{1g} mode eigenvectors are perpendicular to the ab plane and the E_g mode eigenvectors are parallel to the

ab plane. The peaks at 5.0, 6.0, and 6.4 THz can be assigned to the $A_{1g}(\text{Sm})$, $A_{1g}(\text{As})$, and $B_{1g}(\text{Fe})$ mode vibrations, respectively.

Coherent phonons of the iron pnictide $\text{Ba}(\text{Fe}_{1-x}\text{Co}_x)_2\text{As}_2$ have recently been studied by Mansart *et al.*²³⁾ They observed only one coherent A_{1g} mode phonon and suggested that this A_{1g} mode is relevant to the superconducting phase transition. Mertelj *et al.*²⁴⁾ measured transient reflectivity in 50-fs-laser-irradiated $\text{SmFeAsO}_{1-x}\text{F}_x$ ($x=0.2$) to study quasiparticle relaxation and a low-energy electronic structure. They reported a small trace of the $A_{1g}(\text{Sm})$ mode at 5.1 THz. However, the $B_{1g}(\text{Fe})$ mode has not been reported in the iron pnictide superconductors to date. Thus, the present data indicates the first observation of the coherent phonons with the Fe-related mode in the iron oxyphnictide superconductors, as far as we know.

The peak at 5.0 THz exists as a clear asymmetry characteristic with a tail towards the lower frequency. There are two possible reasons for the asymmetric lineshape. One is the overlapping of the weak and broad peaks at frequencies below 5.0 THz, and the other is the frequency chirp of the coherent phonons due to time-dependent phonon–phonon and phonon-carrier couplings.²⁵⁾ However, there are no vibrational modes at around 4.8 THz in the reported Raman and IR spectra and in the density function theory (DFT) calculation.¹¹⁾ The frequency chirp was confirmed using the following analysis with damping oscillations.

A coherent vibration in transient reflection due to coherent phonons is usually analyzed with a combination of damped oscillations for phonons and an exponential decay for electronic response. In the present paper, we used the following equation for the analysis:

$$\begin{aligned} \frac{\Delta R(t)}{R} = & A_1 \exp\left(-\frac{t}{\tau_1}\right) \\ & \times \cos\left\{2\pi\left[\nu_1 + \alpha \exp\left(-\frac{t}{\tau_4}\right)\right]t + \theta_1\right\} \\ & + A_2 \exp\left(-\frac{t}{\tau_2}\right) \cos(2\pi\nu_2 t + \theta_2) \\ & + A_3 \exp\left(-\frac{t}{\tau_3}\right) \cos(2\pi\nu_3 t + \theta_3) \\ & + A_4 \exp\left(-\frac{t}{\tau_4}\right), \end{aligned} \quad (1)$$

where A is the amplitude, τ is the lifetime, ν is the frequency, α is the initial change in frequency, and θ is the initial phase of the oscillation.

The first term of eq. (1) is the damped oscillation including a frequency chirp that represents the asymmetric peak, the second and third terms are usual damped oscillations, and the fourth term is the single exponential decay that represents the electronic contribution. As shown in Fig. 3, the transient reflection signal was well represented using eq. (1) with the parameters listed in Table I. The first term has a frequency of 5.00 THz with an initial change of -0.06 THz (softening). The softening decreases with the delay time, which means that the frequency is positively chirped. The first term corresponds to the $A_{1g}(\text{Sm})$ mode and its lifetime is estimated to be 1.10 ps. The second and third terms have frequencies of 5.91 and 6.34 THz without any chirps and with lifetimes of 0.84 and 1.19 ps, which correspond to the $A_{1g}(\text{As})$ and $B_{1g}(\text{Fe})$ modes, respectively. The FT spectrum obtained from the calculated transient reflection signal using eq. (1) also represents well the experimentally obtained FT spectrum (Fig. 2). The asymmetry of the $A_{1g}(\text{Sm})$ mode peak is most likely due to the positive frequency chirp, which can be explained by the strong carrier–phonon coupling or the anharmonicity of phonons. In the case of the present experiment at low-power excitation with an oscillator laser, the carrier–phonon coupling is more plausible because the anharmonicity plays an important role at high-power excitation with an amplifier laser. When the femtosecond laser irradiates the sample, photoinduced carriers make the atomic bonding weaker via the strong carrier–phonon coupling, resulting in the frequency softening.²⁵⁾ As the delay time increases, the photoinduced carriers relax and the frequency increases. We also measured the transient reflectivity at a higher pump-laser intensity of 110 $\mu\text{J}/\text{cm}^2$ and obtained the frequency of 5.00 THz and the initial frequency change of -0.1 THz. The degree of softening of the initial frequency increases with the photoexcited carrier density. The softening of the frequency is due to both the photoexcited carrier density and characteristic of the excited electronic state, which may be antibonding. At the pump laser intensity of 77 $\mu\text{J}/\text{cm}^2$, the photoexcited carrier density (n_p) was estimated to be $6 \times 10^{19} \text{ cm}^{-3}$, which corresponds to approximately 2% of the carrier density ($n_c \sim 3 \times 10^{21} \text{ cm}^{-3}$)²⁶⁾ and 0.1% of the valence electron density ($n_v = 6 \times 10^{22} \text{ cm}^{-3}$), which is very roughly estimated from the density. The relationship between the electronic softening due to carrier–phonon coupling and n_p was studied experimentally²⁷⁾ and theoretically²⁸⁾ for coherent phonons in Te, which also shows superconductivity at 2.5K at a high pressure of 4 GPa.²⁹⁾ For the A_{1g} mode (3.6 THz) in Te, the electronic softening of 1.4 THz was obtained at $n_p = 0.013n_v$, where $n_v \sim 5 \times 10^{22} \text{ cm}^{-3}$ for Te. Electrons were excited from the bonding state to the antibonding state in Te. Although we do not know details of the photoexcited electronic state in SmAsFeO, if it is an antibonding state similar to that in Te, the electronic softening of 0.1 THz at $n_p = 0.001n_v$ is reasonable. The

frequency chirp due to the carrier–phonon coupling may occur in other phonon modes [$A_{1g}(\text{As})$, $B_{1g}(\text{Fe})$], but the phonon amplitudes are too weak to confirm it.

In summary, the coherent optical phonons of the Fe-related mode $B_{1g}(\text{Fe})$ were first observed at room temperature using femtosecond transient reflection measurements in addition to the $A_{1g}(\text{Sm})$ and $A_{1g}(\text{As})$ modes. The time evolution of the frequency and amplitude of optical phonons was studied and the lifetimes of phonons were estimated. The frequency softening and the positive frequency chirp, which are related to the strong carrier–phonon coupling, were also found in the $A_{1g}(\text{Sm})$ mode. The present experiments show that the coherent phonon measurement is a useful technique for studying the phonon dynamics and carrier–phonon coupling for pnictide superconductors. The measurements of coherent phonons in the superconductive state at low temperatures are now in progress.

Acknowledgments

This work has been partially supported by the X-ray Free Electron Laser Utilization Research Project of the Ministry of Education, Culture, Sports, Science and Technology and Collaborative Research of MSL. We thank Oleg Misochko for valuable discussions.

References

- 1) Y. Kamihara, T. Watanabe, M. Hirano, and H. Hosono: *J. Am. Chem. Soc.* **130** (2008) 3296.
- 2) H. Hiramatsu, T. Katase, T. Kamiya, M. Hirano, and H. Hosono: *Appl. Phys. Lett.* **93** (2008) 162504.
- 3) C. D. L. Cruz, Q. Huang, J. W. Lynn, J. Li, W. Ractliff II, J. L. Zarestky, H. A. Mook, G. F. Chen, J. L. Luo, N. L. Wang, and P. Dai: *Nature* **453** (2008) 899.
- 4) T. Nomura, S. W. Kim, Y. Kamihara, M. Hirano, P. V. Sushko, K. Kato, M. Takata, A. L. Shluger, and H. Hosono: *Supercond. Sci. Technol.* **21** (2008) 125028.
- 5) C. J. Zhang, H. Oyanagi, Z. H. Sun, Y. Kamihara, and H. Hosono: *Phys. Rev. B* **78** (2008) 214513.
- 6) C. Hess, A. Kondrat, A. Narduzzo, J. E. Hamann-Borrero, R. Klingeler, J. Werner, G. Behr, and B. Büchner: *Europhys. Lett.* **87** (2009) 17005.
- 7) Y. Kamihara, T. Nomura, M. Hirano, J. E. Kim, K. Kato, M. Takata, Y. Kobayashi, S. Kitao, S. Higashitaniguchi, Y. Yoda, M. Seto, and H. Hosono: *New. J. Phys.* **12** (2010) 033005.
- 8) J. Yang, Z.-A. Ren, G.-C. Che, W. Lu, X.-L. Shen, Z. C. Li, W. Yi, X.-L. Dong, L.-L. Sun, F. Zhou, and Z.-X. Zhao: *Supercond. Sci. Technol.* **22** (2009) 025004.
- 9) A. P. Litvinchuk, V. G. Hadjiev, M. N. Iliev, B. Lv, A. M. Guloy, and C. W. Chu: *Phys. Rev. B* **78** (2008) 060503(R).
- 10) L. Chauvière, Y. Gallais, M. Cazayous, A. Sacuto, and M. A. Measson: *Phys. Rev. B* **80** (2009) 094504.
- 11) C. Marini, C. Mirri, G. Profeta, S. Lupi, D. Di Castro, R. Soprocase, P. Postorino, P. Calvani, A. Perucchi, S. Massidda, G. M. Tropeano, M. Putti, A. Martinelli, A. Palenzona, and P. Dore: *Europhys. Lett.* **84** (2008) 67013.
- 12) W. Z. Hu, Q. M. Zhang, and N. L. Wang: *Physica C* **469** (2009) 545.
- 13) V. G. Hadjiev, M. N. Iliev, K. Sasmal, Y.-Y. Sun, and C. W. Chu: *Phys. Rev. B* **77** (2008) 220505(R).
- 14) R. H. Liu, T. Wu, G. Wu, H. Chen, X. F. Wang, Y. L. Xie, J. J. Ying, Y. J. Yan, Q. J. Li, B. C. Shi, W. S. Chu, Z. Y. Wu, and X. H. Chen: *Nature* **459** (2009) 64.
- 15) P. M. Shirage, K. Kihou, K. Miyazawa, C.-H. Lee, H. Kito, H. Eisaki, T. Yanagisawa, Y. Tanaka, and A. Iyo: *Phys. Rev. Lett.* **103** (2009) 257003.

- 16) M. Först and T. Dekorsy: in *Coherent Vibrational Dynamics*, ed. S. De Silvestri, G. Cerullo, and G. Lanzani (CRC Press, Boca Raton, FL, 2008) p. 129, and references therein.
- 17) T. Dekorsy, G. C. Cho, and H. Kurz: in *Light Scattering in Solids VIII*, ed. M. Cardona and G. Güntherodt (Springer, Berlin, 2000) p. 180.
- 18) J. M. Chwalek, C. Uher, J. F. Whitaker, G. A. Mourou, J. A. Agostinelli, and M. Levental: [Appl. Phys. Lett. **57** \(1990\) 1696](#).
- 19) W. Albrecht, Th. Kruse, and H. Kurz: [Phys. Rev. Lett. **69** \(1992\) 1451](#).
- 20) O. V. Misochko, K. Kisoda, K. Sakai, and S. Nakashima: [Phys. Rev. B **61** \(2000\) 4305](#).
- 21) O. V. Misochko, N. Georgiev, T. Dekorsy, and M. Helm: [Phys. Rev. Lett. **89** \(2002\) 067002](#).
- 22) H. Takahashi, K. Kato, H. Nakano, M. Kitajima, K. Ohmori, and K. G. Nakamura: [Solid State Commun. **149** \(2009\) 1955](#).
- 23) B. Mansart, D. Boschetto, A. Savoia, F. Rullier-Albenque, A. Forget, D. Colson, A. Rousse, and M. Marsi: [Phys. Rev. B **80** \(2009\) 172504](#).
- 24) T. Mertelj, P. Kusar, V. V. Kabanov, L. Stojchevska, N. D. Zhigadlo, S. Katrych, Z. Bukowski, J. Karpinski, S. Weyeneth, and D. Mihailovic: [Phys. Rev. B **81** \(2010\) 224504](#).
- 25) M. Hase and M. Kitajima: [J. Phys.: Condens. Matter **22** \(2010\) 073201](#).
- 26) M. Tropeano, C. Fanciulli, C. Ferdeghini, D. Marre`, A. S. Siri, M. Putti, A. Martinelli, M. Ferretti, A. Palenzona, M. R. Cimberle, C. Mirri, S. Lupi, R. Sopracase, P. Calvani, and A. Perucchi: [Supercond. Sci. Technol. **22** \(2009\) 034004](#).
- 27) S. Hunsche, K. Wienecke, T. Dekorsy, and H. Kurz: [Phys. Rev. Lett. **75** \(1995\) 1815](#).
- 28) P. Tangney and S. Fahy: [Phys. Rev. Lett. **82** \(1999\) 4340](#).
- 29) F. P. Bundy and K. J. Dunn: [Phys. Rev. Lett. **44** \(1980\) 1623](#).

Table I.

Parameters for eq. (1) for fitting the measured transient reflection signal at pump laser intensity of $77 \mu\text{J}/\text{cm}^2$.

term number	amplitude	life time (ps)	frequency (THz)	initial change (THz)	initial phase (rad)
1	1.04E-6	1.10	5.00	-0.06	2.09
2	3.74E-7	0.84	5.91		2.75
3	0.85E-7	1.19	6.34		1.70
4	1.74E-6	0.47			

Figure Captions

Fig. 1. (Color online)

Transient reflection signal $[\Delta R(t)/R]$ of 40-fs-laser-irradiated $\text{SmFeAsO}_{1-x}\text{F}_x$ ($x = 0.075$). The inset shows oscillation in the signal.

Fig. 2. (Color online)

Fourier transform (FT) spectra of the transient reflection signal from the 40-fs-laser-irradiated $\text{SmFeAsO}_{1-x}\text{F}_x$ ($x = 0.075$). The FT spectrum obtained from the experimental data is shown by small circles. The solid curve shows the FT spectrum from the signal calculated with eq. (1) in the text with parameters listed in Table I.

Fig. 3. (Color online)

Oscillation part of the transient reflection signal in the 40-fs-laser-irradiated $\text{SmFeAsO}_{1-x}\text{F}_x$ ($x = 0.075$). The experimental data is shown by small circles. The solid curve shows a transient reflection signal calculated with eq. (1) in the text with parameters listed in Table I. The red curve indicates the sum of all terms (a), the orange curve indicates term 1 (b), the green curve indicates term 2 (c), and the blue curve indicates term 3 (d).

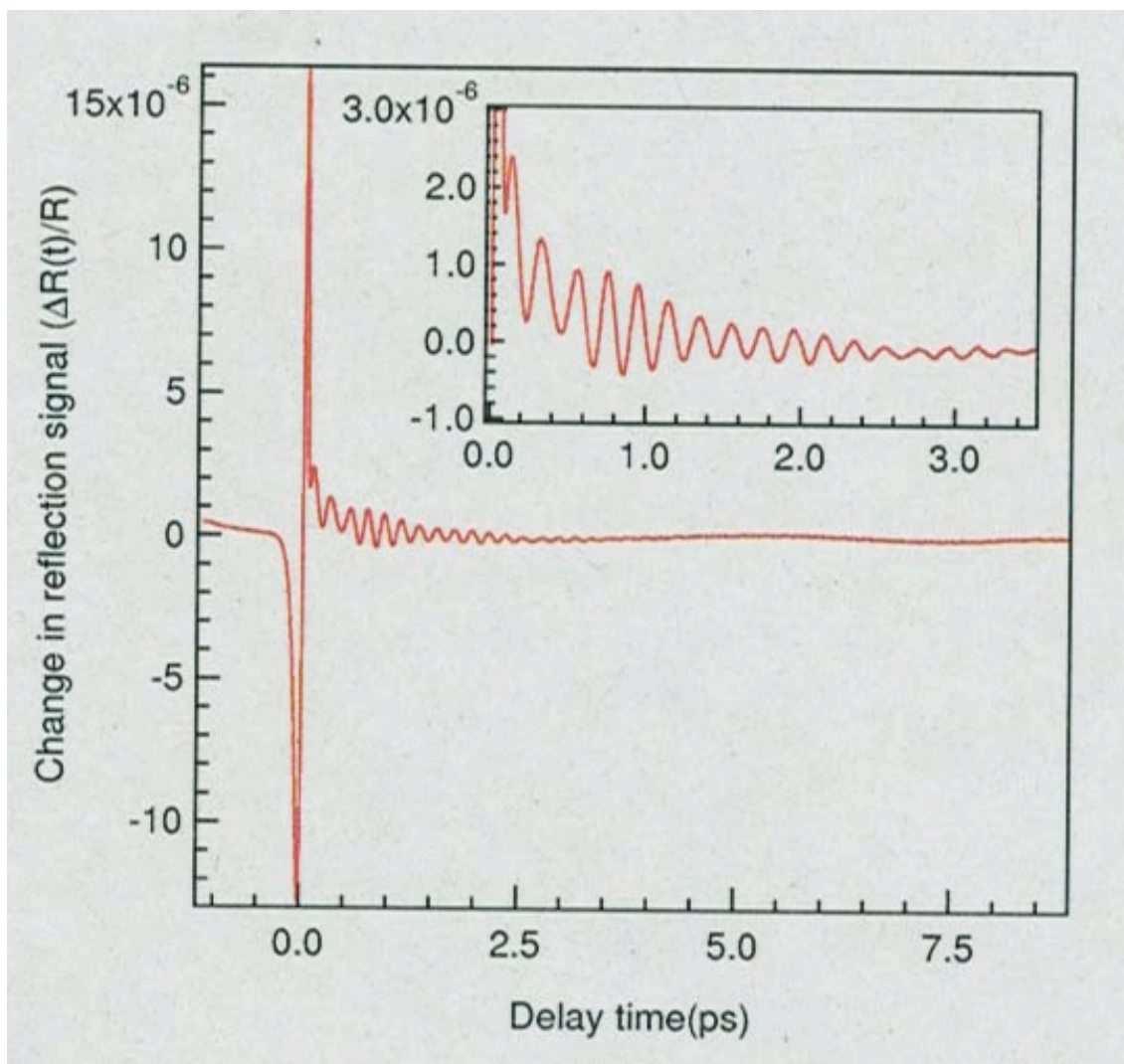


Fig. 1.

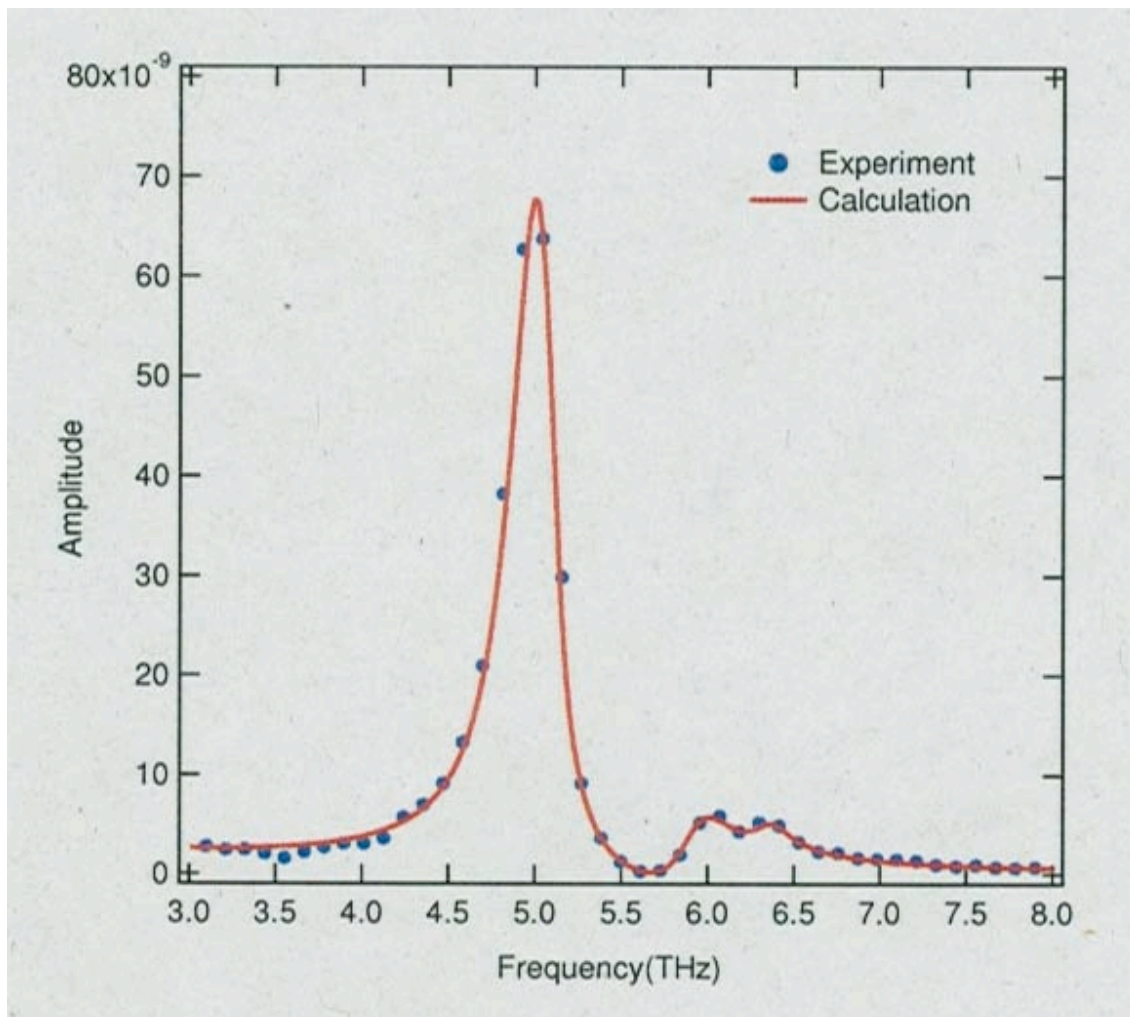


Fig. 2.

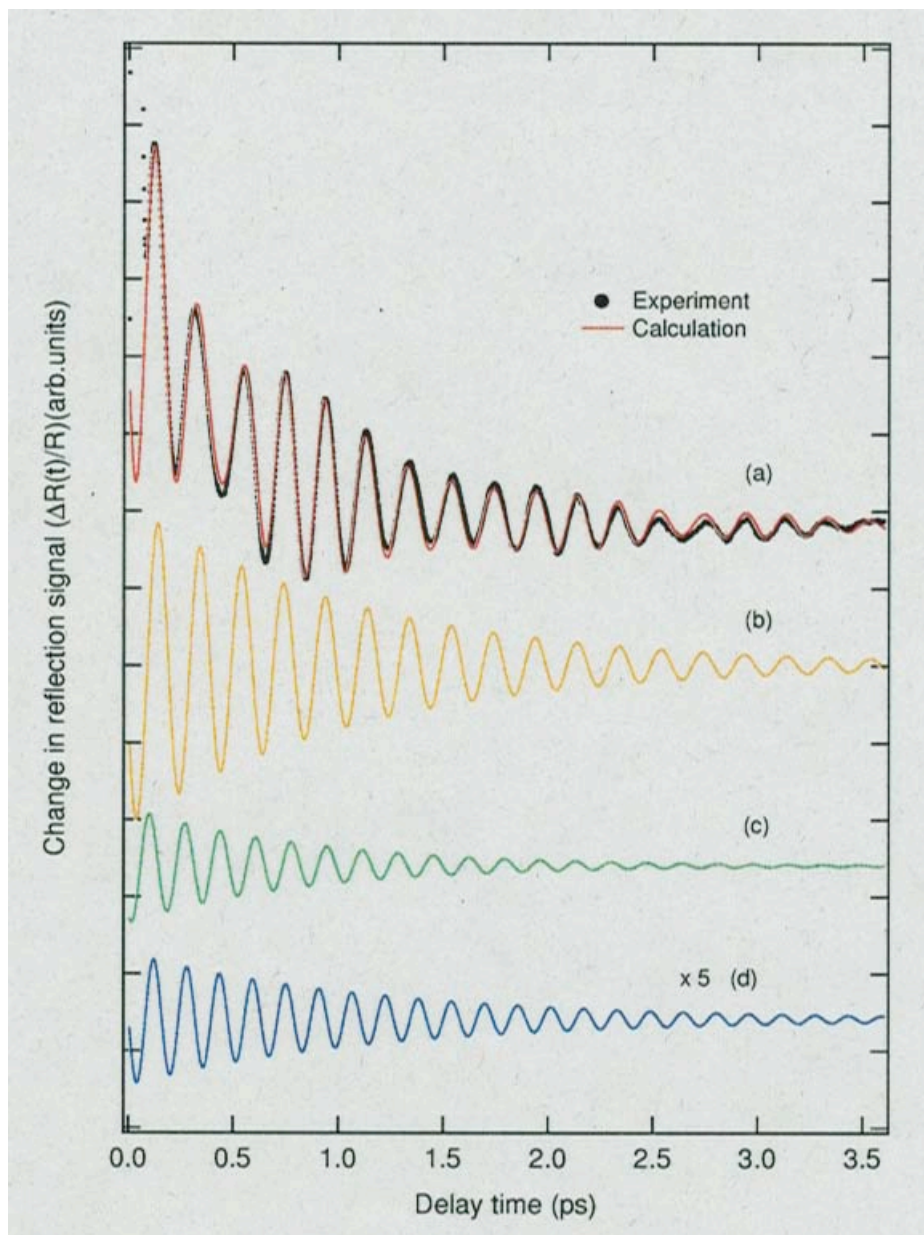


Fig. 3.